

# HumanAesExpert: Advancing a Multi-Modality Foundation Model for Human Image Aesthetic Assessment

Zhichao Liao<sup>1†</sup> Xiaokun Liu<sup>2</sup> Wenyu Qin<sup>2</sup> Qingyu Li<sup>2</sup> Qiulin Wang<sup>2</sup>  
Pengfei Wan<sup>2</sup> Di Zhang<sup>2</sup> Long Zeng<sup>1✉</sup> Pingfa Feng<sup>1</sup>

<sup>1</sup>Tsinghua University <sup>2</sup>Kuaishou Technology

<https://humanaesexpert.github.io/HumanAesExpert/>

## Abstract

Image Aesthetic Assessment (IAA) is a long-standing and challenging research task. However, its subset, Human Image Aesthetic Assessment (HIAA), has been scarcely explored, even though HIAA is widely used in social media, AI workflows, and related domains. To bridge this research gap, our work pioneers a holistic implementation framework tailored for HIAA. Specifically, we introduce **HumanBeauty**, the first dataset purpose-built for HIAA, which comprises 108k high-quality human images with manual annotations. To achieve comprehensive and fine-grained HIAA, 50K human images are manually collected through a rigorous curation process and annotated leveraging our trailblazing 12-dimensional aesthetic standard, while the remaining 58K with overall aesthetic labels are systematically filtered from public datasets. Based on the **HumanBeauty** database, we propose **HumanAesExpert**, a powerful Vision Language Model for aesthetic evaluation of human images. We innovatively design an Expert head to incorporate human knowledge of aesthetic sub-dimensions while jointly utilizing the Language Modeling (LM) and Regression head. This approach empowers our model to achieve superior proficiency in both overall and fine-grained HIAA. Furthermore, we introduce a MetaVoter, which aggregates scores from all three heads, to effectively balance the capabilities of each head, thereby realizing improved assessment precision. Extensive experiments demonstrate that our **HumanAesExpert** models deliver significantly better performance in HIAA than other state-of-the-art models. Our datasets, models, and codes are publicly released to advance the HIAA community.

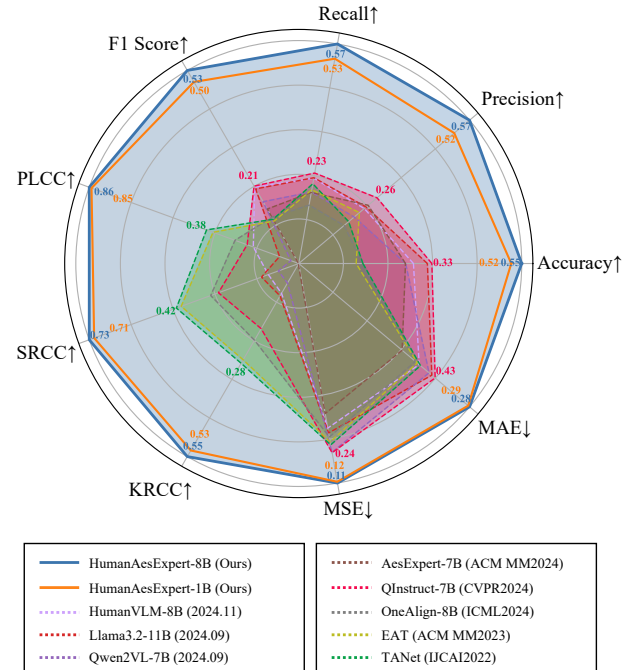


Figure 1. **Our HumanAesExpert, compared to existing state-of-the-art methods, shows exceptional improvements.** ↑ indicates that larger values are better, while ↓ signifies the opposite.

## 1. Introduction

Human Image Aesthetic Assessment (HIAA) extends traditional Image Aesthetic Assessment (IAA) [5, 8, 38, 52, 55] by shifting focus to quantitative evaluation of human-centric images. It aims to systematically analyze aesthetic dimensions (e.g., facial features, body shape, environment) to assign measurable scores, transforming subjective human visual appeal into objective computational metrics. HIAA demonstrates extensive applicability across domains, such as employing quantitative aesthetic analysis to optimize content curation in social media recommendation sys-

<sup>†</sup> Work done during internship at KwaiVGI, Kuaishou Technology.

✉ Corresponding author.

tems, and implementing measurable quality metrics in generative AI workflows [28, 32] to refine human-centered synthetic imagery. However, HIAA has not been explicitly explored in previous work. Recently, benefiting from the outstanding performance of Vision Language Models (VLMs) [12, 33, 34, 43, 45] in multimodal tasks, VLM-based IAA methods [21, 48, 49, 58] have secured significant breakthroughs. Nevertheless, as shown in Fig. 1, general IAA approaches exhibit suboptimal performance when handling specialized HIAA tasks, severely restricting the practical application of HIAA. Consequently, it is urgent to develop a holistic framework capable of conducting systematic and professional aesthetic assessments for human-centric images (HIAA) to bridge these critical research gaps.

Diverse and informative human image data with aesthetic labels are essential for HIAA. However, to our knowledge, there is no open-source HIAA dataset in existence. To address the data gap, we introduce **HumanBeauty**, the first dataset dedicated to HIAA research. We first employ face detection algorithms [7] to curate 58,564 human images from public IAA datasets [15, 25, 27, 30, 38, 54] and unify their aesthetic score scales. Notably, these data exhibit two significant shortcomings in achieving comprehensive and fine-grained HIAA: **1) Image level:** Insufficient human images with poor coverage of HIAA attributes (e.g., numerous images contain only facial or head regions, neglecting full-body aesthetics). **2) Annotation level:** Only overall aesthetic scores, with the absence of sub-dimensional granular annotations supported by a systematic aesthetic standard. To resolve these issues, guided by extensive consultations with aesthetic experts and studio professionals, we establish a 12-dimensional HIAA standard that encompasses all critical attributes of HIAA. Based on this standard, we implement an iterative training-testing protocol to train annotators. Ultimately, we organize 368 certified volunteers to collect 50,022 informative human images from the Internet, with each image undergoing rigorous multi-dimensional manual annotation following our aesthetic standard. Integrating data from both phases, we build our HumanBeauty dataset, which contains a total of 108k annotated human images and is the largest HIAA dataset compared to existing related datasets, as shown in Tab. 1.

Current VLM-based IAA methods have demonstrated promising efficacy, they predominantly adopt two architectural paradigms as shown in Fig. 2: (a) LM head-based VLMs: Methods [46, 48, 49, 58] discretize continuous scores into textual labels (e.g., “good” and “bad”) for training, and then map predictions back to scores via softmax probabilities during inference. However, supervision with discrete labels hinders the accurate fitting of continuous scores. (b) Regression head-based VLMs: Approaches [18, 31] replace LM heads with Regression heads to predict Mean Opinion Scores (MOS) directly. While mitigat-

Table 1. Comparisons with existing related datasets.

| Dataset                   | Publication Year | Human / Total            | Theme        |
|---------------------------|------------------|--------------------------|--------------|
| Gray et al. [11]          | 2010             | 2,056 / 2,056            | Face         |
| AVA [38]                  | 2012             | 44,920 / 255,530         | General      |
| SCUT-FBP 5500 [30]        | 2018             | 5,500 / 5,500            | Face         |
| MEBeauty [25]             | 2022             | 2,550 / 2,550            | Face         |
| ICAA17K [16]              | 2023             | 3894 / 17,726            | Color        |
| BAID [54]                 | 2023             | 13,869 / 60,337          | Artistic     |
| AGIQA [27]                | 2023             | 1218 / 2,982             | AI-Generated |
| AesBench [22]             | 2024             | 894 / 2,800              | General      |
| AesMMIT [21]              | 2024             | 5179 / 21,904            | General      |
| <b>HumanBeauty (Ours)</b> | <b>2025</b>      | <b>108,586 / 108,586</b> | <b>Human</b> |

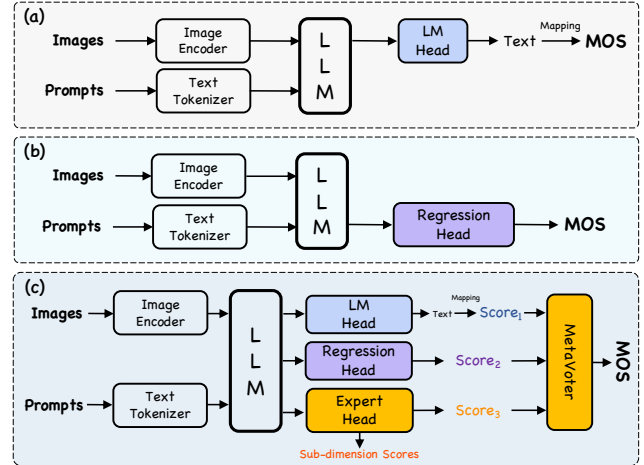


Figure 2. **Model comparison with the most related works:** (a) LM head-based VLM, fine-tuned on IAA datasets without changing the original architecture. (b) Regression head-based VLM, which replaces the LM head with a Regression head. (c) Our approach uses both heads along with an Expert head and MetaVoter.

ing discretization errors, it sacrifices the text comprehension proficiency of large language models (LLMs), reducing interpretability. Moreover, learning multi-dimensional aesthetic scores via a single Regression head risks distribution conflicts and domain-specific accuracy degradation. Therefore, to simultaneously enable granular aesthetic evaluation and preserve the model’s text comprehension capabilities with scoring precision, we propose **HumanAesExpert**, which introduces an Expert head to integrate fine-grained aesthetic knowledge, working in tandem with the LM head and Regression head. Furthermore, we design a MetaVoter that aggregates scores from three heads to generate the final scores, which employs learnable weights to balance the contributions of each head, improving the aesthetic assessment accuracy. Finally, we conduct extensive experiments to demonstrate that our approach achieves state-of-the-art performance (SOTA) in HIAA compared to previous works. In summary, our contributions are as follows:

- To our knowledge, we are the pioneering work for HIAA and introduce the **HumanBeauty** dataset, which is the

first large-scale dataset dedicated to HIAA, comprising 108K manually annotated human images.

- We propose the **HumanAesExpert**, a foundation VLM for HIAA, which innovatively introduces an Expert Head and MetaVoter to achieve fine-grained aesthetic evaluation and balance contributions of multi heads.
- Extensive experiments demonstrate that our models achieve SOTA performance in HIAA across all metrics.
- We publicly release our datasets, models, and codes to drive the development of the HIAA community.

## 2. Related Works

**Image Aesthetic Assessment Datasets.** The most popular and largest general IAA dataset is the AVA dataset [38]. Over the years, AVA has significantly advanced the development of the IAA community. It has also served as the source dataset for several subsequent datasets, including recent works like AesBench [22] and AesExpert [21]. However, general IAA often lacks clear scoring criteria, leading to discrepancies in aesthetic evaluation points that human raters focus on. This results in abnormal score distributions and data quality decline. Given the extensive application of facial attractiveness in psychology, datasets [11, 25, 30] using facial beauty as a scoring criterion have been continuously developed. While ICAA17K [16] focuses on image color, BAID [54] on artistic IAA, and AGIQA [27] on AI-generated images, as summarized in Tab. 1, there remains a lack of open-source datasets centered on human subjects. Such datasets should consider not only facial beauty but also factors like body shape, environment, and more.

**Traditional Assessment Methods.** Traditional assessment methods involve using Convolutional Neural Networks (CNN) [13, 24, 40, 42, 50] or Vision Transformers (ViT) [9, 14, 36, 39] to extract image features and predict scores using a Regression head. CNN-based methods [15, 19], pre-trained on ImageNet [6], have been extensively studied. However, these methods often lose the prior knowledge of pre-training in the fine-tuning process, limiting the models’ ability to understand aesthetics and effectively identify salient regions. In addition, achieving human-level aesthetic alignment requires priors comparable to humans. CNNs and ViTs pre-trained on ImageNet fall short of this objective, and there remains a lack of causal reasoning. The models do not understand which factors contribute to the overall aesthetic scores.

**VLM-based Assessment Methods.** Compared to traditional assessment methods, VLMs like GPT-4 [2] exhibit strong causal reasoning capabilities. Recent works, such as Q-Bench [47], Q-Align [48], and UNIAA-LLaVA [58], propose mapping scores to discrete text-defined levels, which are used to fine-tune VLMs. During inference, the softmax function is applied to the logits of the rating-level words corresponding to the score token to derive scores. However,

this approach fails to leverage the continuous supervisory signal from the scores. To better utilize this signal, works [18, 31] replace the LM head with a Regression head. However, the LM head is a critical component for causal reasoning in LLMs, and removing it leads to similar issues observed in traditional assessment methods [46]. In addition, this method struggles with cross-dimension data. Specifically, scores from different domains are learned through the same Regression head, resulting in information coupling that hinders proper fitting for domain-specific tasks.

## 3. HumanBeauty Dataset Construction

Our HumanBeauty Dataset is composed of two segments: HumanBeauty-58k and HumanBeauty-50k. In this section, we will detail the construction process of each segment.

### 3.1. HumanBeauty-58K

Although existing IAA datasets cannot completely meet our task requirements, they include a moderate number of human images with overall aesthetic scores, which are capable of improving the model’s overall assessment ability, robustness, and dataset diversity. Following prior works [21, 47], we collect 58k relevant human images from public datasets.

**Datasets Selection.** Firstly, adhering to ethical principles, we only consider open-source datasets free of gore, violence, and other harmful content. Secondly, as IAA presents cross-domain and out-of-domain challenges, it is vital to incorporate diverse types of human images, such as natural, artistic, and AI-generated images. Thirdly, given the application distribution of downstream tasks, we primarily focus on natural human images. Motivated by the above considerations, we ultimately select SCUT-FBP 5500 [30], MEBeauty [25], AVA [38], TAD66K [15], BAID [54], and AGIQA [27] as our data sources, shown in Fig. 3 (a).

**Data Filtration.** Due to the significant impact of facial aesthetics on HIAA, it necessitates that human images cover facial regions as thoroughly as possible. Similar to LAION-FACE [57], FLIP-80M [29] and HumanVLM [4], we also use RetinaFace [7], a face detection algorithm, to filter human-related data from general datasets, shown in Fig. 3 (b). Since single-human IAA underpins multi-human interaction analysis, we curate our dataset to include only single-face images, ensuring methodological continuity for future multi-human studies. Eventually, we collect 58,564 human images, which are suitable for our task.

**Normalization.** Owing to varying aesthetic score scales across datasets, we unify them to [0,1] using Min-Max normalization, as defined by the following equation:

$$y_i = \frac{x_i - \min(x)}{\max(x) - \min(x)}, \quad (1)$$

where  $x$  is a set of filtered dataset scores, and  $y$  is the normalized score. Each dataset is independently normalized.

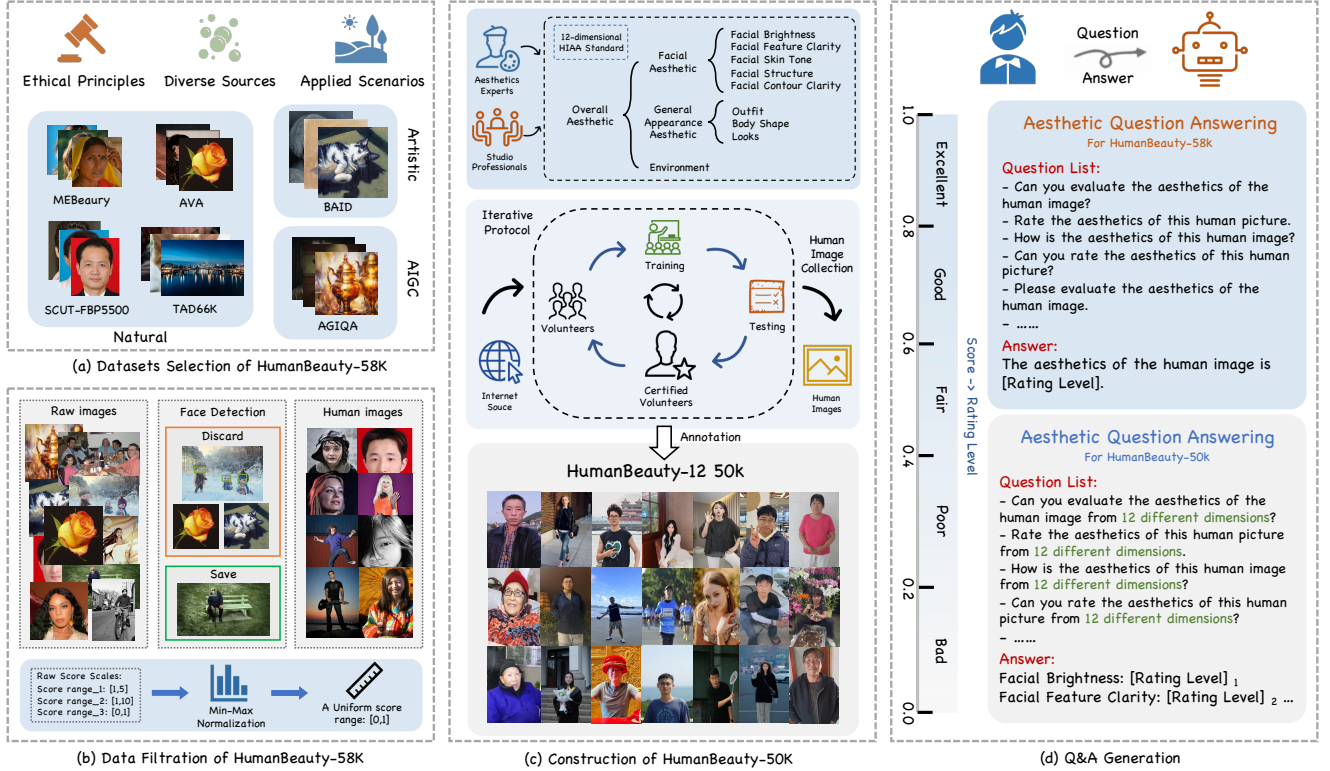


Figure 3. **Our HumanBeauty dataset construction pipeline.** First, we select six diverse open-source datasets as data sources and perform data filtering to build our HumanBeauty-58k. Additionally, we manually collect and annotate 50k high-quality human images with nuanced 12-dimensional aesthetic annotations. The process is shown in Fig. 3 (c). Finally, we map all the scores into text of rating level to form QA pairs for training.

### 3.2. HumanBeauty-50K

To address the limitations of **Annotation level** and **Image level** in open-source data for achieving comprehensive and fine-grained HIAA, we additionally collect 50k high-quality human images with nuanced 12-dimensional aesthetic annotations. The process is shown in Fig. 3 (c).

**12-dimensional HIAA Standard.** Due to the inherently subjective and vague nature of aesthetics, individuals exhibit significant differences in their evaluations and often lack concrete criteria to justify their judgments. Motivated by the desire to reconcile aesthetic disparities among individuals and establish a systematic and attributable assessment standard, we collect extensive opinions from aesthetics experts and studio professionals, summarized as follows: **1)** The standard should cover all critical aspects that affect HIAA. **2)** The standard should be hierarchical and attributable, with the attributes of the smallest sub-dimensions being decoupled from each other and directly contributing to their parent dimensions. **3)** The facial region has a significant impact on HIAA and requires more fine-grained evaluation dimensions. **4)** The general appearance and environment are equally important for the overall aesthetics. Based on these, we establish the 12-dimensional

aesthetic assessment standard for HIAA, which is similar to the sub-dimensional decomposition methodology in IAA, as illustrated in Fig. 3 (c). The standard includes three groups: **1)** Facial aesthetic: facial brightness, facial feature clarity, facial skin tone, facial structure, and facial contour clarity. **2)** General appearance aesthetic: outfit, body shape, and looks. **3)** Environment. These sub-dimensions simultaneously contribute to the overall aesthetic.

**Iterative Protocol.** Our dataset construction is highly professional and challenging. To ensure data quality, we design a rigorous Iterative Training-Testing Protocol to qualify our volunteers. Specifically, we invite 455 volunteers from various fields, and aesthetic experts train them on human image collection principles and scoring criteria based on the 12-dimensional HIAA standard. Volunteers undergo qualification tests, with those failing to meet requirements exiting the project, while the qualified proceed to subsequent phases of training and testing in an iterative manner. Ultimately, 368 certified volunteers are retained to collect and annotate human images for our dataset. Notably, we periodically repeat this protocol during the formal image collection and annotation process to ensure a high-quality dataset.

**Human Image Collection.** We organize the certified volunteers to collect human images following the principles



below: **1)** Exclusion of ethical violations (e.g., privacy, explicit or violent content). Note that all non-public individual images in the manuscript have been authorized. **2)** Images should focus on the face while including body representation of the subject (excluding portraits that focus solely on the face/head). **3)** Images could contain multiple individuals, but must feature a single dominant human subject. Ultimately, we collect 50,022 human images from the Internet. **Aesthetic Annotation.** We organize the certified volunteers to annotate the collected human images across 12 dimensions. Each dimension is scored within the range [0,1], and each image is annotated by at least 9 raters. The final score for each dimension is the Mean Opinion score (MOS), calculated as the average of all raters’ scores.

### 3.3. Question Answer Generation

To meet the requirements of QA training pairs in VLMs and rating-level text supervision for the LM head [48], we convert the scores in existing datasets into discrete rating-level text. Inspired by Q-Align [48] and UNIAA [58], we divide the scores into five equal intervals and map them to discrete text labels using a piecewise function:

$$Z(s) = z_i, \text{ if } \frac{z-1}{5} < s \leq \frac{z}{5}, \quad (2)$$

where  $\{z_i\}_{i=1}^5 = \{bad, poor, fair, good, excellent\}$ , defined by ITU [41], are standard text of rating levels.

As shown in Fig. 3 (d), for HumanBeauty-58K, we randomly select a question from a group of paraphrases [48] and directly map the overall aesthetics score to rating level as the answer, to construct QA pair, e.g.:

- **Question:** *Rate the aesthetics of this human picture.*
- **Answer:** *The aesthetics of the image is [Rating Level].*

For HumanBeauty-50K, we also select a question about 12-dimensional HIAA from a set of conditional paraphrases and map the scores of each sub-dimension to rating levels, assembling the answer in the format: [Sub-dimension Name]: [Rating level]<sub>n</sub>, where  $n \in [1, 12]$ . For example:

- **Question:** *Can you evaluate the aesthetics of the human image from 12 different dimensions?*
- **Answer:** *Facial Brightness: [Rating level]<sub>1</sub>  
Facial Feature Clarity: [Rating Level]<sub>2</sub> ...*

## 4. HumanAesExpert Model

In this section, we introduce the **HumanAesExpert** model. It employs both the LM head and the Regression head to leverage their respective strengths: text comprehension and continuous score learning. However, a single Regression head is unable to learn scores from different dimensions across domains, like the overall scores from HumanBeauty-58K and the 12-dimensional scores from HumanBeauty-50K. Additionally, it cannot reflect the hierarchical structure of our 12-dimensional aesthetic assessment standard.

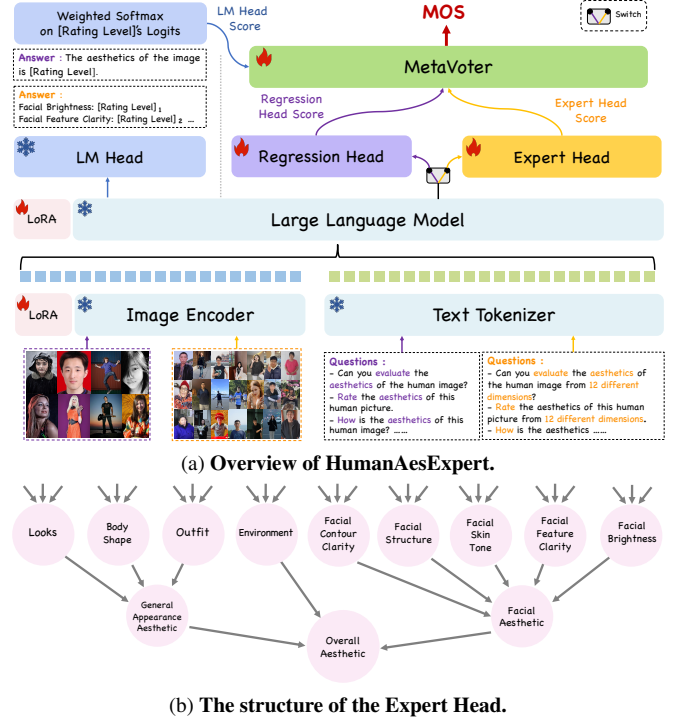


Figure 4. (a) The training path of the human images with only overall annotations and 12-dimensional annotations are highlighted with purple and yellow, respectively. (b) The Expert head is a sparsely connected MLP, with each node being supervised.

To address this issue, we innovatively introduce the Expert head to integrate the knowledge of aesthetic sub-dimension, achieving fine-grained HIAA. Moreover, we propose a MetaVoter to combine the capabilities of these heads. This approach allows the three heads to collaboratively determine the final score.

Next, we will introduce each of these components individually. Given an image  $x$  and a text prompt  $p$ , we can obtain the final layer output  $h = M(x, p)$  of the VLM model  $M$ , which will be fed to different heads.

**LM Head.** The LM head  $H_{LM}$  [48, 58], typically a linear layer, is used to obtain the logits  $l = H_{LM}(h)$  for all words in the vocabulary. During training, these logits are used to compute the cross-entropy loss with the ground truth:

$$\mathcal{L}_{Entropy} = -\frac{1}{N} \sum_{n=1}^N \sum_{i=1}^L y_{(i,n)} \log(l_{(i,n)}), \quad (3)$$

where  $N$  is the length of the ground truth answer,  $L$  is the length of the vocabulary, and  $y \in \{0, 1\}$ . During inference, the logits  $p$  of the  $\{bad, poor, fair, good, excellent\}$  are extracted from the logits  $l$ , and the weighted softmax function is applied to get a numerical score. The formula is

defined as follows:

$$S_{LM} = \sum_{i=1}^5 \frac{i \cdot e^p}{\sum_{j=1}^5 e^p}. \quad (4)$$

**Regression Head.** Denoted as  $H_{reg}$  [18, 46], directly obtain scores  $S_{reg} = H_{reg}(h)$  via the last token (I.e. the class token) and use Mean Squared Error (MSE) loss to supervise the model learning, as shown in the following equation:

$$\mathcal{L}_{reg} = \frac{1}{N} \sum_{n=1}^N (\bar{y} - S_{reg})^2, \quad (5)$$

where  $N$  is the number of assessment dimensions, and  $\bar{y}$  is the ground truth scores.

**Expert Head.** Our Expert head  $H_{exp}$  uses a sparsely connected MLP to replicate the relationships between scoring dimensions. Specifically, the first layer is a linear layer that directly derives the 9 smallest dimensional scores, depicted in Fig. 4 (b). The general appearance aesthetic score and the facial aesthetic score are obtained from their corresponding smallest dimensional scores using two Feed-Forward Networks (FFNs). Finally, another FFN is used to integrate the environment score with the two parent dimensional scores to achieve the overall aesthetic score. We apply MSE loss to each node to ensure the expected specific score learning. The Expert head can be used to generate 12-dimensional scores  $score_1, \dots, score_{12} = H_{exp}(h)$ .

**MetaVoter.** To balance the contributions of multiple heads, an additional MLP with batch normalization and ReLU activation functions, termed the Metavoter  $V$ , is trained to aggregate scores from the three heads for the final prediction:  $y_{final} = V(S'_{LM}, S_{reg}, S_{exp})$ , where  $S'_{LM}$  is the normalized  $S_{LM}$  using Min-Max normalization, and  $S_{exp} = score_{12}$ . Mean Absolute Error (MAE) loss is used to supervise the learning of MetaVoter  $V$ , formulated as follows:

$$\mathcal{L}_{MetaVoter} = \frac{1}{N} \sum_{n=1}^N |\bar{y} - V(S'_{LM}, S_{reg}, S_{exp})|, \quad (6)$$

where  $N$  is the batch size.

**Training.** As illustrated in Fig. 4 (a). Our method employs a two-stage training. In the first stage, we fine-tune the VLM and train the newly added Regression and Expert heads. Similar to our data, our training includes two types: 1) Only overall annotation: The VLM processes the question, while the image encoder handles the human image from HumanBeauty-58K. The LM head and Regression head are optimized using the overall aesthetics scores and rating levels. 2) 12-dimensional annotations: The VLM receives a conditional question, and the image encoder processes the human images from HumanBeauty-50K. The LM

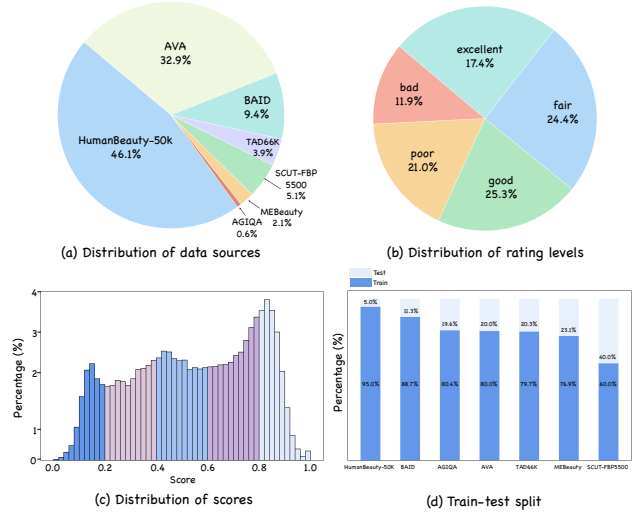


Figure 5. Statistical analysis and train-test split.

head and Expert head are trained on the 12-dimensional rating levels and corresponding scores. We design a switch between the Regression head and Expert head to control gradient flow and prevent cross-domain conflicts. Thus, our loss function is formulated as follows:

$$\mathcal{L}_{LLM} = \begin{cases} \mathcal{L}_{Entropy} + \lambda \cdot \mathcal{L}_{reg} & f = 0 \\ \mathcal{L}_{Entropy} + \mu \cdot \mathcal{L}_{exp} & f = 1 \end{cases}, \quad (7)$$

where  $\lambda, \mu$  are loss balancing terms,  $\mathcal{L}_{exp}$  represents the same MSE loss as  $\mathcal{L}_{reg}$ , and  $f$  indicates the data case type. In the second stage, we freeze all model components except for the MetaVoter and optimize the MetaVoter using the scores from the three heads according to Eq. 6.

## 5. Experiments

### 5.1. Statistical Analysis and Experimental Setup

**Statistical Analysis.** We present the distribution of our dataset in Fig. 5 (a), showing that natural images constitute the majority, with artistic images accounting for 9.4% and AIGC images comprising 0.6%. This distribution aligns with practical application scenarios of HIAA. In Fig. 5 (b) and (c), we illustrate the distributions of rating levels and scores. The balanced rating levels and the fact that no 0.02 score interval exceeds 4% demonstrate the diversity of our data and the effectiveness of the annotation process.

**Train-Test Split.** To ensure the balance of the test set, we split the data from the subsets of HumanBeauty by reasonable proportions, shown in Fig. 5 (d). The training set comprises 94,099 human images, while the test set contains 14,487 human images.

**Implementation Details.** We provide two model variants: 1) HumanAesExpert-1B, consisting of Qwen2-0.5B [51]

Table 2. **Comparison with SOTA methods.**  $\uparrow$  represents the larger is the better, while  $\downarrow$  represents smaller is the better. The upper part of the table lists traditional IAA methods, which use CNN or ViT. The lower part of the table consists of VLM methods. **Bold** indicates the best, and underline indicates the second best.

| Method                   | Publication | MSE $\downarrow$ | MAE $\downarrow$ | PLCC $\uparrow$ | SRCC $\uparrow$ | KRCC $\uparrow$ | Accuracy $\uparrow$ | Precision $\uparrow$ | Recall $\uparrow$ | F1 Score $\uparrow$ |
|--------------------------|-------------|------------------|------------------|-----------------|-----------------|-----------------|---------------------|----------------------|-------------------|---------------------|
| TANet [15]               | IJCAI2022   | 0.2684           | 0.4905           | 0.3799          | 0.4240          | 0.2820          | 0.1576              | 0.1667               | 0.2052            | 0.1224              |
| CLIPQA+ [44]             | AAAI2023    | 0.2207           | 0.4259           | 0.2999          | 0.3112          | 0.2117          | 0.2954              | 0.2272               | 0.2164            | 0.1666              |
| VILA [23]                | CVPR2023    | 0.2844           | 0.5031           | 0.2521          | 0.3055          | 0.2139          | 0.1666              | 0.1605               | 0.1864            | 0.1352              |
| EAT [17]                 | ACM MM2023  | 0.2803           | 0.5036           | 0.3533          | 0.4073          | 0.2722          | 0.1410              | 0.2027               | 0.1900            | 0.1174              |
| QualiCLIP [3]            | ArXiv2403   | 0.2575           | 0.4409           | 0.2877          | 0.2146          | 0.1435          | 0.3296              | 0.2394               | 0.2270            | 0.2195              |
| OneAlign-8B [48]         | ICML2024    | 0.3000           | 0.5117           | 0.2626          | 0.3051          | 0.2168          | 0.1569              | 0.1515               | 0.1502            | 0.1280              |
| QInstruct-7B [49]        | CVPR2024    | 0.2367           | 0.4290           | 0.2125          | 0.2783          | 0.1841          | 0.3270              | 0.2616               | 0.2328            | 0.2138              |
| LLaVA1.6-7B [35]         | Blog2401    | 0.2538           | 0.4239           | 0.2272          | 0.1312          | 0.1025          | 0.2813              | 0.1712               | 0.1820            | 0.1590              |
| Phi3.5-4B [1]            | ArXiv2404   | 0.2723           | 0.4398           | 0.1321          | 0.1937          | 0.1452          | 0.2387              | 0.2184               | 0.1948            | 0.1651              |
| AesExpert-7B [21]        | ACM MM2024  | 0.3947           | 0.5674           | 0.0008          | 0.0033          | 0.0021          | 0.2622              | 0.2319               | 0.1830            | 0.1505              |
| Glm-4v-9b [10]           | ArXiv2406   | 0.2965           | 0.4785           | 0.0843          | 0.0329          | 0.0281          | 0.2133              | 0.1891               | 0.2114            | 0.1450              |
| InternVL2-1B [43]        | Blog2407    | 0.3985           | 0.5716           | 0.0001          | 0.0221          | 0.0179          | 0.2779              | 0.1970               | 0.1972            | 0.1916              |
| InternVL2-8B [43]        | Blog2407    | 0.3324           | 0.5006           | 0.0001          | 0.0229          | 0.0157          | 0.2809              | 0.2015               | 0.2014            | 0.1958              |
| LLaVAov-1B [26]          | ArXiv2408   | 0.2448           | 0.4181           | 0.0201          | 0.0416          | 0.0339          | 0.3413              | 0.0948               | 0.1987            | 0.1074              |
| MiniCPM2.6-8B [53]       | ArXiv2408   | 0.2656           | 0.4348           | 0.0541          | 0.0859          | 0.0626          | 0.3167              | 0.1851               | 0.1968            | 0.1745              |
| Qwen2VL-7B [45]          | ArXiv2409   | 0.2383           | 0.4546           | 0.0323          | 0.0708          | 0.0551          | 0.2626              | 0.1851               | 0.1840            | 0.1706              |
| Llama3.2-11B [37]        | Blog2409    | 0.3165           | 0.4429           | 0.0791          | 0.1291          | 0.0916          | 0.3160              | 0.2250               | 0.2208            | 0.2061              |
| HumanVLM-8B [4]          | ArXiv2411   | 0.3359           | 0.4958           | 0.1873          | 0.1054          | 0.0844          | 0.2818              | 0.2189               | 0.2196            | 0.2109              |
| <b>HumanAesExpert-1B</b> | –           | 0.1194           | 0.2906           | 0.8539          | 0.7090          | 0.5286          | 0.5221              | 0.5195               | 0.5273            | 0.5016              |
| <b>HumanAesExpert-8B</b> | –           | <b>0.1141</b>    | <b>0.2849</b>    | <b>0.8632</b>   | <b>0.7259</b>   | <b>0.5459</b>   | <b>0.5478</b>       | <b>0.5707</b>        | <b>0.5652</b>     | <b>0.5334</b>       |

Table 3. **Comparison on fine-grained HIAA**, where MAE are reported, and “G-A Aesthetic” denotes general appearance aesthetic.

| Method                   | Facial Brightness | Facial Feature Clarity | Facial Skin Tone | Facial Structure | Facial Contour Clarity | Facial Aesthetic  |
|--------------------------|-------------------|------------------------|------------------|------------------|------------------------|-------------------|
| OneAlign-8B [48]         | 0.7501            | 0.4882                 | 0.5995           | 0.4886           | 0.3880                 | 0.3110            |
| QInstruct-7B [49]        | 0.4324            | 0.6597                 | 0.4582           | 0.4576           | 0.6168                 | 0.4482            |
| LLaVA1.6-7B [35]         | 0.5781            | 0.6589                 | 0.4701           | 0.5735           | 0.5688                 | 0.5095            |
| HumanVLM-8B [4]          | 0.7830            | 0.7380                 | 0.5775           | 0.7204           | 0.7184                 | 0.5916            |
| <b>HumanAesExpert-1B</b> | <u>0.3209</u>     | <u>0.3943</u>          | <u>0.3949</u>    | <u>0.3718</u>    | <u>0.3415</u>          | <u>0.2920</u>     |
| <b>HumanAesExpert-8B</b> | <b>0.3028</b>     | <b>0.3113</b>          | <b>0.3242</b>    | <b>0.3413</b>    | <b>0.3101</b>          | <b>0.2412</b>     |
| Method                   | Outfit            | Body Shape             | Looks            | G-A Aesthetic    | Environment            | Overall Aesthetic |
| OneAlign-8B [48]         | 0.4153            | 0.3506                 | 0.3232           | 0.3526           | 0.3367                 | 0.5117            |
| QInstruct-7B [49]        | 0.2996            | 0.3384                 | 0.4228           | 0.4054           | 0.5082                 | 0.4290            |
| LLaVA1.6-7B [35]         | 0.4320            | 0.5043                 | 0.4765           | 0.4268           | 0.5409                 | 0.4239            |
| HumanVLM-8B [4]          | 0.5030            | 0.6538                 | 0.5193           | 0.5365           | 0.5844                 | 0.4958            |
| <b>HumanAesExpert-1B</b> | <u>0.2918</u>     | <u>0.2728</u>          | <u>0.2512</u>    | <u>0.2986</u>    | <u>0.2910</u>          | <u>0.2906</u>     |
| <b>HumanAesExpert-8B</b> | <b>0.1803</b>     | <b>0.2704</b>          | <b>0.2471</b>    | <b>0.2671</b>    | <b>0.2708</b>          | <b>0.2849</b>     |

and InternViT-300M [43]. 2) HumanAesExpert-8B, consisting of InternLM2-7B and InternViT-300M. VLM fine-tuning is conducted by the SWIFT framework [56] with LoRA [20] on V100 GPUs, while newly added modules are initialized and trained from scratch. To prevent overfitting, the epoch of the first training stage is set to 1, while MetaVoter is trained for 10 epochs in the second stage.

**Evaluation Metrics.** We evaluate the score prediction capabilities of models using several metrics: MSE and MAE measure the distance between the model’s predicted scores

and the ground truth (GT) scores, reflecting alignment with human aesthetics. Pearson Linear Correlation Coefficient (PLCC), Spearman Rank Correlation Coefficient (SRCC), and Kendall Rank Correlation Coefficient (KRCC) assess the correlation between the model’s predictions and the GT scores. Accuracy, mean Precision, mean Recall, and mean F1 Score compare the model’s predicted rating levels with those mapped from the GT scores.

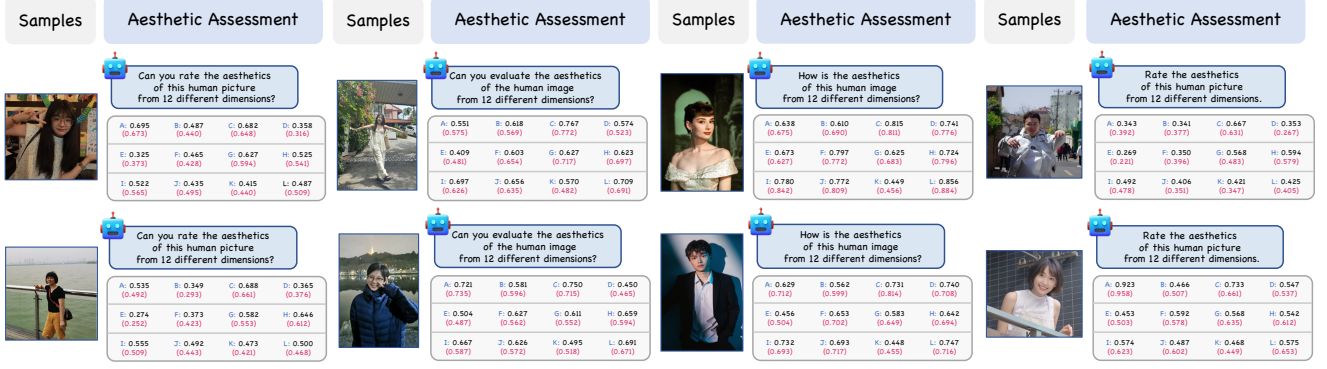


Figure 6. **The Visualization Results of Our Model**, where “( )” indicate the Ground Truth scores. From A to L, they respectively represent facial brightness, facial feature clarity, facial skin tone, facial structure, facial contour clarity, facial aesthetic, outfit, body shape, looks, general appearance aesthetic, environment and overall aesthetic scores.

## 5.2. Quantitative and Qualitative Evaluation

**Quantitative Evaluation.** We conduct a quantitative comparison of overall HIAA and fine-grained HIAA against existing SOTA methods on our test set. For overall HIAA, we compare with the latest open-source methods as baselines from two main categories: traditional CNN and ViT models [3, 15, 17, 23, 44], and VLM-based methods [1, 4, 10, 21, 26, 35, 37, 43, 45, 48, 49, 53]. The results, as shown in Tab. 2, demonstrate that our HumanAesExpert-8B and HumanAesExpert-1B achieve the optimal and suboptimal performance across all metrics. Concretely, our 1B and 8B models outperform TANet [15] (the best among other methods), achieving 124% and 127% gains in PLCC, 74% and 78% in SRCC, and 87% and 94% in KRCC, respectively. For fine-grained HIAA, we select the top four methods in Tab. 2 and assess them across our 12 aesthetic dimensions. We report the MAE metric in Tab. 3, which measures the distance between predicted scores and GT, providing more intuitive evidence of alignment with human aesthetic judgment. Our models consistently achieve the best and second-best results across all sub-dimensions. Specifically, compared to QInstruct-7B [49], our 1B and 8B models reduce MAE by 26% and 30% on the face brightness sub-dimension and by 19% and 25% on the face structure sub-dimension, respectively. Similarly, compared to OneAlign-8B [48], our models achieve reductions of 22% and 23% on the looks sub-dimension. These results support the proposed Expert head in achieving fine-grained HIAA learning via a hierarchical sparsely connected network structure. In summary, the exceptional improvements of our model in both overall and fine-grained HIAA tasks demonstrate the effectiveness of our holistic framework.

**Qualitative Evaluation.** We design a qualitative evaluation by simulating the model usage process. We ask our model to perform aesthetic evaluations on human images across 12 dimensions and directly compare the outputs with

the ground truth. As shown in Fig. 6, the evaluation results of our model closely match human aesthetic annotations, indicating a high level of aesthetic consistency with human judgments. In the first image, due to hair occlusion obscuring the facial contour, the model assigns a lower score to this dimension. These observations demonstrate the model’s capability in fine-grained HIAA. In the fourth image, a notably low overall aesthetic score is observed, attributed to equally low scores in both general appearance aesthetics and facial aesthetics. Further analysis reveals deficiencies in facial brightness, clarity of facial features, and contour definition. This aligns with our intuitive observation: the facial features of the person appear less distinct due to his heavier build. By systematically tracing back from the total score, we identify the underlying factors that contribute to the low evaluation, demonstrating that our established assessment standard is inherently attributable.

## 5.3. Ablation Study

In the ablation study, we randomly selected 138 images from each sub-dataset in the test set to create a balanced quick test set. Inspired by VideoScore [18], we use InternVL2-1B and InternVL2-8B [43], fine-tuned with only the Regression head, as our baselines. As shown in Tab. 4, when we add the LM head, the model performance nearly doubles since the LM head guides the learning of all tokens. Adding our proposed Expert head further boosts the model’s performance significantly, as the hierarchical neural network design aligns with the evaluation standard, which enhances VLM’s understanding of human aesthetics. Finally, incorporating our proposed MetaVoter yields the best results, indicating that deriving the final score from multiple heads is effective.



Table 4. Ablation Study on Our Proposed Modules.

| Model Modules |         |          |           | HumanAesExpert-1B |               |              | HumanAesExpert-8B |               |               |
|---------------|---------|----------|-----------|-------------------|---------------|--------------|-------------------|---------------|---------------|
| Reg-Head      | LM-Head | Exp-Head | MetaVoter | PLCC ↑            | SRCC ↑        | KRCC ↑       | PLCC ↑            | SRCC ↑        | KRCC ↑        |
| ✓             |         |          |           | 0.1841            | 0.1716        | 0.1176       | 0.2173            | 0.1802        | 0.1144        |
| ✓             | ✓       |          |           | 0.4122            | 0.3943        | 0.2666       | 0.4809            | 0.454         | 0.3804        |
| ✓             | ✓       | ✓        |           | 0.621             | 0.5456        | 0.377        | 0.7153            | 0.7075        | 0.5047        |
| ✓             | ✓       | ✓        | ✓         | <b>0.7627</b>     | <b>0.7483</b> | <b>0.562</b> | <b>0.7968</b>     | <b>0.7804</b> | <b>0.5965</b> |

## 6. Conclusion

In this paper, we introduce the HumanBeauty dataset with the guidance of our 12-dimensional human aesthetic evaluation standard, which contains 108K images with real annotations, and the HumanAesExpert series of models featuring our proposed Expert head and MetaVoter module. Our experiments demonstrate that our methods achieve state-of-the-art performance on this dataset. Nevertheless, our models still underperform on some metrics, reflecting that our dataset is highly challenging and far from being saturated. Furthermore, we validate the effectiveness of our proposed modules. Our dataset, models, and code are open-sourced, potentially establishing our work as a foundation for HIAA.

## References

- [1] Marah Abdin, Jyoti Aneja, Hany Awadalla, Ahmed Awadallah, Ammar Ahmad Awan, Nguyen Bach, Amit Bahree, Arash Bakhtiari, Jianmin Bao, Harkirat Behl, et al. Phi-3 technical report: A highly capable language model locally on your phone. *arXiv preprint arXiv:2404.14219*, 2024. 7, 8
- [2] Josh Achiam, Steven Adler, Sandhini Agarwal, Lama Ahmad, Ilge Akkaya, Florencia Leoni Aleman, Diogo Almeida, Janko Altenschmidt, Sam Altman, Shyamal Anadkat, et al. Gpt-4 technical report. *arXiv preprint arXiv:2303.08774*, 2023. 3
- [3] Lorenzo Agnolucci, Leonardo Galteri, and Marco Bertini. Quality-aware image-text alignment for real-world image quality assessment. *arXiv preprint arXiv:2403.11176*, 2024. 7, 8
- [4] Dawei Dai, Xu Long, Li Yutang, Zhang Yuanhui, and Shuyin Xia. HumanVLM: Foundation for human-scene vision-language model. *arXiv preprint arXiv:2411.03034*, 2024. 3, 7, 8
- [5] Maedeh Daryanavard Chounchenani, Asadollah Shahbahrami, Reza Hassanpour, and Georgi Gaydadjiev. Deep learning based image aesthetic quality assessment-a review. *ACM Computing Surveys*, 2024. 1
- [6] Jia Deng, Wei Dong, Richard Socher, Li-Jia Li, Kai Li, and Li Fei-Fei. Imagenet: A large-scale hierarchical image database. In *2009 IEEE conference on computer vision and pattern recognition*, pages 248–255. Ieee, 2009. 3
- [7] Jiankang Deng, Jia Guo, Evangelos Ververas, Irene Kotisia, and Stefanos Zafeiriou. Retinaface: Single-shot multi-level face localisation in the wild. In *Proceedings of the IEEE/CVF conference on computer vision and pattern recognition*, pages 5203–5212, 2020. 2, 3
- [8] Yubin Deng, Chen Change Loy, and Xiaoou Tang. Image aesthetic assessment: An experimental survey. *IEEE Signal Processing Magazine*, 34(4):80–106, 2017. 1
- [9] Alexey Dosovitskiy. An image is worth 16x16 words: Transformers for image recognition at scale. *arXiv preprint arXiv:2010.11929*, 2020. 3
- [10] Team GLM, Aohan Zeng, Bin Xu, Bowen Wang, Chenhui Zhang, Da Yin, Dan Zhang, Diego Rojas, Guanyu Feng, Hanlin Zhao, et al. Chatglm: A family of large language models from glm-130b to glm-4 all tools. *arXiv preprint arXiv:2406.12793*, 2024. 7, 8
- [11] Douglas Gray, Kai Yu, Wei Xu, and Yihong Gong. Predicting facial beauty without landmarks. In *Computer Vision—ECCV 2010: 11th European Conference on Computer Vision, Heraklion, Crete, Greece, September 5–11, 2010, Proceedings, Part VI 11*, pages 434–447. Springer, 2010. 2, 3
- [12] Daya Guo, Dejian Yang, Haowei Zhang, Junxiao Song, Ruoyu Zhang, Runxin Xu, Qihao Zhu, Shirong Ma, Peiyi Wang, Xiao Bi, et al. Deepseek-r1: Incentivizing reasoning capability in llms via reinforcement learning. *arXiv preprint arXiv:2501.12948*, 2025. 2
- [13] Kaiming He, Xiangyu Zhang, Shaoqing Ren, and Jian Sun. Deep residual learning for image recognition. In *Proceedings of the IEEE conference on computer vision and pattern recognition*, pages 770–778, 2016. 3
- [14] Kaiming He, Xinlei Chen, Saining Xie, Yanghao Li, Piotr Dollár, and Ross Girshick. Masked autoencoders are scalable vision learners. In *Proceedings of the IEEE/CVF conference on computer vision and pattern recognition*, pages 16000–16009, 2022. 3
- [15] Shuai He, Yongchang Zhang, Rui Xie, Dongxiang Jiang, and Anlong Ming. Rethinking image aesthetics assessment: Models, datasets and benchmarks. In *IJCAI*, pages 942–948, 2022. 2, 3, 7, 8
- [16] Shuai He, Anlong Ming, Yaqi Li, Jinyuan Sun, ShunTian Zheng, and Huadong Ma. Thinking image color aesthetics assessment: Models, datasets and benchmarks. In *Proceedings of the IEEE/CVF International Conference on Computer Vision*, pages 21838–21847, 2023. 2, 3
- [17] Shuai He, Anlong Ming, Shuntian Zheng, Haobin Zhong, and Huadong Ma. Eat: An enhancer for aesthetics-oriented transformers. In *Proceedings of the 31st ACM International Conference on Multimedia*, pages 1023–1032, 2023. 7, 8
- [18] Xuan He, Dongfu Jiang, Ge Zhang, Max Ku, Achint Soni, Sherman Siu, Haonan Chen, Abhranil Chandra, Ziyang Jiang, Aaran Arulraj, et al. Videoscore: Building automatic metrics to simulate fine-grained human feedback for video generation. *arXiv preprint arXiv:2406.15252*, 2024. 2, 3, 6, 8
- [19] Vlad Hosu, Bastian Goldlücke, and Dietmar Saupe. Effective aesthetics prediction with multi-level spatially pooled features. In *proceedings of the IEEE/CVF conference on computer vision and pattern recognition*, pages 9375–9383, 2019. 3
- [20] Edward J Hu, Yelong Shen, Phillip Wallis, Zeyuan Allen-Zhu, Yuanzhi Li, Shean Wang, Lu Wang, and Weizhu Chen.

- Lora: Low-rank adaptation of large language models. *arXiv preprint arXiv:2106.09685*, 2021. 7
- [21] Yipo Huang, Xiangfei Sheng, Zhichao Yang, Quan Yuan, Zhichao Duan, Pengfei Chen, Leida Li, Weisi Lin, and Guangming Shi. Aesexpert: Towards multi-modality foundation model for image aesthetics perception. In *Proceedings of the 32nd ACM International Conference on Multimedia*, pages 5911–5920, 2024. 2, 3, 7, 8
- [22] Yipo Huang, Quan Yuan, Xiangfei Sheng, Zhichao Yang, Haoning Wu, Pengfei Chen, Yuzhe Yang, Leida Li, and Weisi Lin. Aesbench: An expert benchmark for multimodal large language models on image aesthetics perception. *arXiv preprint arXiv:2401.08276*, 2024. 2, 3
- [23] Junjie Ke, Keren Ye, Jiahui Yu, Yonghui Wu, Peyman Milanfar, and Feng Yang. Vila: Learning image aesthetics from user comments with vision-language pretraining. In *Proceedings of the IEEE/CVF Conference on Computer Vision and Pattern Recognition*, pages 10041–10051, 2023. 7, 8
- [24] Alex Krizhevsky, Ilya Sutskever, and Geoffrey E Hinton. Imagenet classification with deep convolutional neural networks. *Advances in neural information processing systems*, 25, 2012. 3
- [25] Irina Lebedeva, Yi Guo, and Fangli Ying. Mebeauty: a multi-ethnic facial beauty dataset in-the-wild. *Neural Computing and Applications*, pages 1–15, 2022. 2, 3
- [26] Bo Li, Yuanhan Zhang, Dong Guo, Renrui Zhang, Feng Li, Hao Zhang, Kaichen Zhang, Peiyuan Zhang, Yanwei Li, Ziwei Liu, et al. Llava-onevision: Easy visual task transfer. *arXiv preprint arXiv:2408.03326*, 2024. 7, 8
- [27] Chunyi Li, Zicheng Zhang, Haoning Wu, Wei Sun, Xiongkuo Min, Xiaohong Liu, Guangtao Zhai, and Weisi Lin. Agiqa-3k: An open database for ai-generated image quality assessment. *IEEE Transactions on Circuits and Systems for Video Technology*, 2023. 2, 3
- [28] Xinghui Li, Qichao Sun, Pengze Zhang, Fulong Ye, Zhichao Liao, Wanquan Feng, Songtao Zhao, and Qian He. Any-dressing: Customizable multi-garment virtual dressing via latent diffusion models. *arXiv preprint arXiv:2412.04146*, 2024. 2
- [29] Yudong Li, Xianxu Hou, Zheng Dezhi, Linlin Shen, and Zhe Zhao. Flip-80m: 80 million visual-linguistic pairs for facial language-image pre-training. In *Proceedings of the 32nd ACM International Conference on Multimedia*, pages 58–67, 2024. 3
- [30] Lingyu Liang, LuoJun Lin, Lianwen Jin, Duorui Xie, and Mengru Li. Scut-fbp5500: A diverse benchmark dataset for multi-paradigm facial beauty prediction. In *2018 24th International conference on pattern recognition (ICPR)*, pages 1598–1603. IEEE, 2018. 2, 3
- [31] Youwei Liang, Junfeng He, Gang Li, Peizhao Li, Arseniy Klimovskiy, Nicholas Carolan, Jiao Sun, Jordi Pont-Tuset, Sarah Young, Feng Yang, et al. Rich human feedback for text-to-image generation. In *Proceedings of the IEEE/CVF Conference on Computer Vision and Pattern Recognition*, pages 19401–19411, 2024. 2, 3
- [32] Ente Lin, Xujie Zhang, Fuwei Zhao, Yuxuan Luo, Xin Dong, Long Zeng, and Xiaodan Liang. Dreamfit: Garment-centric human generation via a lightweight anything-dressing encoder. *arXiv preprint arXiv:2412.17644*, 2024. 2
- [33] Aixin Liu, Bei Feng, Bing Xue, Bingxuan Wang, Bochao Wu, Chengda Lu, Chenggang Zhao, Chengqi Deng, Chenyu Zhang, Chong Ruan, et al. Deepseek-v3 technical report. *arXiv preprint arXiv:2412.19437*, 2024. 2
- [34] Haotian Liu, Chunyuan Li, Yuheng Li, and Yong Jae Lee. Improved baselines with visual instruction tuning. In *Proceedings of the IEEE/CVF Conference on Computer Vision and Pattern Recognition*, pages 26296–26306, 2024. 2
- [35] Haotian Liu, Chunyuan Li, Yuheng Li, Bo Li, Yuanhan Zhang, Sheng Shen, and Yong Jae Lee. Llava-next: Improved reasoning, ocr, and world knowledge. <https://llava-vl.github.io/blog/2024-01-30-llava-next>, 2024. 7, 8
- [36] Ze Liu, Yutong Lin, Yue Cao, Han Hu, Yixuan Wei, Zheng Zhang, Stephen Lin, and Baining Guo. Swin transformer: Hierarchical vision transformer using shifted windows. In *Proceedings of the IEEE/CVF international conference on computer vision*, pages 10012–10022, 2021. 3
- [37] Meta. Llama-3.2-11b-vision. <https://ai.meta.com/blog/llama-3-2-connect-2024-vision-edge-mobile-devices>, 2024. 7, 8
- [38] Naila Murray, Luca Marchesotti, and Florent Perronnin. Ava: A large-scale database for aesthetic visual analysis. In *2012 IEEE conference on computer vision and pattern recognition*, pages 2408–2415. IEEE, 2012. 1, 2, 3
- [39] Alec Radford, Jong Wook Kim, Chris Hallacy, Aditya Ramesh, Gabriel Goh, Sandhini Agarwal, Girish Sastry, Amanda Askell, Pamela Mishkin, Jack Clark, et al. Learning transferable visual models from natural language supervision. In *International conference on machine learning*, pages 8748–8763. PMLR, 2021. 3
- [40] Mark Sandler, Andrew Howard, Menglong Zhu, Andrey Zhmoginov, and Liang-Chieh Chen. Mobilenetv2: Inverted residuals and linear bottlenecks. In *Proceedings of the IEEE conference on computer vision and pattern recognition*, pages 4510–4520, 2018. 3
- [41] B Series. Methodology for the subjective assessment of the quality of television pictures. *Recommendation ITU-R BT*, 500(13), 2012. 5
- [42] Karen Simonyan and Andrew Zisserman. Very deep convolutional networks for large-scale image recognition. *arXiv preprint arXiv:1409.1556*, 2014. 3
- [43] OpenGVLab Team. Internvl2: Better than the best—expanding performance boundaries of open-source multimodal models with the progressive scaling strategy. <https://internvl.github.io/blog/2024-07-02-internvl-2.0>, 2024. 2, 7, 8
- [44] Jianyi Wang, Kelvin CK Chan, and Chen Change Loy. Exploring clip for assessing the look and feel of images. In *Proceedings of the AAAI Conference on Artificial Intelligence*, pages 2555–2563, 2023. 7, 8
- [45] Peng Wang, Shuai Bai, Sinan Tan, Shijie Wang, Zhihao Fan, Jinze Bai, Keqin Chen, Xuejing Liu, Jialin Wang, Wenbin Ge, et al. Qwen2-vl: Enhancing vision-language model’s perception of the world at any resolution. *arXiv preprint arXiv:2409.12191*, 2024. 2, 7, 8

- [46] Yibin Wang, Zhiyu Tan, Junyan Wang, Xiaomeng Yang, Cheng Jin, and Hao Li. Lift: Leveraging human feedback for text-to-video model alignment. *arXiv preprint arXiv:2412.04814*, 2024. 2, 3, 6
- [47] Haoning Wu, Zicheng Zhang, Erli Zhang, Chaofeng Chen, Liang Liao, Annan Wang, Chunyi Li, Wenxiu Sun, Qiong Yan, Guangtao Zhai, et al. Q-bench: A benchmark for general-purpose foundation models on low-level vision. *arXiv preprint arXiv:2309.14181*, 2023. 3
- [48] Haoning Wu, Zicheng Zhang, Weixia Zhang, Chaofeng Chen, Liang Liao, Chunyi Li, Yixuan Gao, Annan Wang, Erli Zhang, Wenxiu Sun, et al. Q-align: Teaching lmms for visual scoring via discrete text-defined levels. *arXiv preprint arXiv:2312.17090*, 2023. 2, 3, 5, 7, 8
- [49] Haoning Wu, Zicheng Zhang, Erli Zhang, Chaofeng Chen, Liang Liao, Annan Wang, Kaixin Xu, Chunyi Li, Jingwen Hou, Guangtao Zhai, et al. Q-instruct: Improving low-level visual abilities for multi-modality foundation models. In *Proceedings of the IEEE/CVF Conference on Computer Vision and Pattern Recognition*, pages 25490–25500, 2024. 2, 7, 8
- [50] Saining Xie, Ross Girshick, Piotr Dollár, Zhuowen Tu, and Kaiming He. Aggregated residual transformations for deep neural networks. In *Proceedings of the IEEE conference on computer vision and pattern recognition*, pages 1492–1500, 2017. 3
- [51] An Yang, Baosong Yang, Beichen Zhang, Binyuan Hui, Bo Zheng, Bowen Yu, Chengyuan Li, Dayiheng Liu, Fei Huang, Haoran Wei, et al. Qwen2. 5 technical report. *arXiv preprint arXiv:2412.15115*, 2024. 6
- [52] Hongtao Yang, Ping Shi, Saike He, Da Pan, Zefeng Ying, and Ling Lei. A comprehensive survey on image aesthetic quality assessment. In *2019 IEEE/ACIS 18th International Conference on Computer and Information Science (ICIS)*, pages 294–299. IEEE, 2019. 1
- [53] Yuan Yao, Tianyu Yu, Ao Zhang, Chongyi Wang, Junbo Cui, Hongji Zhu, Tianchi Cai, Haoyu Li, Weilin Zhao, Zhihui He, et al. Minicpm-v: A gpt-4v level mllm on your phone. *arXiv preprint arXiv:2408.01800*, 2024. 7, 8
- [54] Ran Yi, Haoyuan Tian, Zhihao Gu, Yu-Kun Lai, and Paul L Rosin. Towards artistic image aesthetics assessment: a large-scale dataset and a new method. In *Proceedings of the IEEE/CVF Conference on Computer Vision and Pattern Recognition*, pages 22388–22397, 2023. 2, 3
- [55] Jiajing Zhang, Yongwei Miao, and Jinhui Yu. A comprehensive survey on computational aesthetic evaluation of visual art images: Metrics and challenges. *IEEE Access*, 9:77164–77187, 2021. 1
- [56] Yuze Zhao, Jintao Huang, Jinghan Hu, Xingjun Wang, Yunlin Mao, Daoze Zhang, Zeyinzi Jiang, Zhikai Wu, Baole Ai, Ang Wang, et al. Swift: a scalable lightweight infrastructure for fine-tuning. *arXiv preprint arXiv:2408.05517*, 2024. 7
- [57] Yinglin Zheng, Hao Yang, Ting Zhang, Jianmin Bao, Dongdong Chen, Yangyu Huang, Lu Yuan, Dong Chen, Ming Zeng, and Fang Wen. General facial representation learning in a visual-linguistic manner. In *Proceedings of the IEEE/CVF conference on computer vision and pattern recognition*, pages 18697–18709, 2022. 3
- [58] Zhaokun Zhou, Qiulin Wang, Bin Lin, Yiwei Su, Rui Chen, Xin Tao, Amin Zheng, Li Yuan, Pengfei Wan, and Di Zhang. Uniaa: A unified multi-modal image aesthetic assessment baseline and benchmark. *arXiv preprint arXiv:2404.09619*, 2024. 2, 3, 5